Redox Biology 69 (2024) 103019

Contents lists available at ScienceDirect

Redox Biology

journal homepage: www.elsevier.com/locate/redox

Bile duct ligation elevates 5-HT levels in cerebral cortex of rats partly due to impairment of brain UGT1A6 expression and activity via ammonia accumulation

Hanyu Yang [a,b,1], Linjun You [c,1], Zhongyan Wang [b,1], Lu Yang [b], Xun Wang [b], Wenhan Wu [b], Hao Zhi [b], Guangmei Rong [b], Yun Sheng [b], Xiaodong Liu [a,b,**], Li Liu [a,b,*]

[a] State Key Laboratory of Natural Medicines, Key Laboratory of Drug Metabolism and Pharmacokinetics, China Pharmaceutical University, 210009, Nanjing, China
[b] Department of Pharmacology, School of Pharmacy, China Pharmaceutical University, Nanjing, 210009, China
[c] Center for New Drug Safety Evaluation and Research, China Pharmaceutical University, 210009, Nanjing, China

ARTICLE INFO

Keywords:
Hepatic encephalopathy
Serotonin
UDP-Glucuronosyltransferase 1A6
Ammonia
Reactive oxygen species
Hepatocyte nuclear factor 4α

ABSTRACT

Hepatic encephalopathy (HE) is often associated with endogenous serotonin (5-HT) disorders. However, the reason for elevated brain 5-HT levels due to liver failure remains unclear. This study aimed to investigate the mechanism by which liver failure increases brain 5-HT levels and the role in behavioral abnormalities in HE. Using bile duct ligation (BDL) rats as a HE model, we verified the elevated 5-HT levels in the cortex but not in the hippocampus and striatum, and found that this cortical 5-HT overload may be caused by BDL-mediated inhibition of UDP-glucuronosyltransferase 1A6 (UGT1A6) expression and activity in the cortex. The intraventricular injection of the UGT1A6 inhibitor diclofenac into rats demonstrated that the inhibition of brain UGT1A6 activity significantly increased cerebral 5-HT levels and induced HE-like behaviors. Co-immunofluorescence experiments demonstrated that UGT1A6 is primarily expressed in astrocytes. In vitro studies confirmed that NH_4Cl activates the ROS-ERK pathway to downregulate UGT1A6 activity and expression in U251 cells, which can be reversed by the oxidative stress antagonist N-acetyl-L-cysteine and the ERK inhibitor U0126. Silencing Hepatocyte Nuclear Factor 4α (HNF4α) suppressed UGT1A6 expression whilst overexpressing HNF4α increased Ugt1a6 promotor activity. Meanwhile, both NH_4Cl and the ERK activator TBHQ downregulated HNF4α and UGT1A6 expression. In the cortex of hyperammonemic rats, we also found activation of the ROS-ERK pathway, decreases in HNF4α and UGT1A6 expression, and increases in brain 5-HT content. These results prove that the ammonia-mediated ROS-ERK pathway activation inhibits HNF4α expression to downregulate UGT1A6 expression and activity, thereby increasing cerebral 5-HT content and inducing manic-like HE symptoms. This is the first study to reveal the mechanism of elevated cortical 5-HT concentration in a state of liver failure and elucidate its association with manic-like behaviors in HE.

1. Introduction

Acute and chronic liver failure is often associated with behavioral abnormalities and compromised cognition and is termed hepatic encephalopathy (HE). Approximately 50–70 % of patients with liver failure exhibit HE syndromes [1,2]. The main hypothesis suggests that HE is attributable to neurocyte damage caused by the accumulation of neurotoxic substances [1–4]. However, the clinical syndromes of most patients with HE are reversible, and no obvious nerve damage occurs in the brains of these patients [5], suggesting that other mechanisms contribute to behavioral abnormalities and cognition impairment in patients with HE.

Abnormal alterations in levels of brain neurotransmitters such as dopamine (DA) and serotonin (5-HT) contribute to some neurological and psychiatric disorders [6,7]. HE is often accompanied by disorders of

* Corresponding author. State Key Laboratory of Natural Medicines, Key Laboratory of Drug Metabolism and Pharmacokinetics, China Pharmaceutical University, 210009, Nanjing, China.
** Corresponding author. State Key Laboratory of Natural Medicines, Key Laboratory of Drug Metabolism and Pharmacokinetics, China Pharmaceutical University, 210009, Nanjing, China.
E-mail addresses: xdliu@cpu.edu.cn (X. Liu), liulee@cpu.edu.cn (L. Liu).
[1] These authors equally contributed to this work.

https://doi.org/10.1016/j.redox.2023.103019
Received 27 September 2023; Received in revised form 19 December 2023; Accepted 27 December 2023
Available online 28 December 2023

Abbreviations

5-HT	Serotonin
5-HIAA	5-hydroxyindoleacetic acid
5-HTP	5-Hydroxytryptophan
5-HT-G	5-HT glucuronide conjugate
AhR	Aryl Hydrocarbon Receptor
BBB	Blood-Brain Barrier
BDL	Bile Duct Ligation
CAR	Constitutive Androstane Receptor
CNS	Central Nervous System
DA	Dopamine
DIC	Diclofenac Sodium
ERK	Extracellular Signal-Regulated Kinase
HA	Hyperammonemia
HE	Hepatic Encephalopathy
HNF4α	Hepatocyte Nuclear Factor 4α
MAO	Monoamine Oxidase
NAC	N-acetyl-L-cysteine
Nrf2	NR-E2-related factor 2
PNPG	4-nitrophenyl β-D-glucuronide
PXR	Pregnane X Receptor
ROS	Reactive Oxygen Species
SERT	Serotonin transporter
TPH2	Tryptophan hydroxylase 2
UCB	Unconjugated bilirubin
UGT1A6	UDP-glucuronosyltransferase 1A6

the neurotransmitters in the brain. Borg et al. reported that the levels of DA, histamine, gamma-aminobutyric acid, and 5-HT in the cerebrospinal fluid of patients with HE were significantly higher than those in controls [8]. Our previous study also reported significantly increased DA levels in the cortex of bile duct ligation (BDL) rats, partly attributed to tyrosine hydroxylase upregulation [9]. Furthermore, our preliminary experiment showed that BDL significantly increased 5-HT levels in the prefrontal cortex of rats, accompanied by behavioral abnormalities. Notably, an increased level of brain 5-HT or the excessive activation of brain 5-HT receptors by drugs can lead to a series of central nervous system (CNS) symptoms, including akathisia, anxiety, delirium, neuromuscular rigidity, and even coma, known as serotonin syndrome [10]. The clinical symptoms of HE are similar to those of the serotonin syndrome, indicating that increased levels of brain 5-HT induced by BDL also contribute to the occurrence of HE.

5-HT is found throughout the body. However, because of the blood-brain barrier (BBB), the synthesis and metabolism of 5-HT in the CNS and periphery are relatively independent [11]. Tryptophan hydroxylase 2 (TPH2) is the rate-limiting enzyme in 5-HT biosynthesis [12], and TPH2 polymorphisms are associated with anxiety phenotypes [13]. Monoamine oxidases (MAO-A and MAO-B) are key enzymes in the classical 5-HT metabolic pathway, which metabolizes 5-HT to 5-hydroxyindoleacetic acid (5-HIAA). We found that BDL time-dependently altered the expression of MAO-A proteins in the cortices of BDL rats: the expression of cortex MAO-A in 14-day BDL rats was decreased but increased in 28-day BDL, whilst the expression of cortex MAO-B protein was unaffected by BDL [9]. Autopsy reports demonstrated that both MAO-A and MAO-B activities were significantly increased in brain tissue from patients with cirrhosis who died of hepatic coma [14]; however, another report showed that MAO-A activity was increased, but MAO-B activity was unchanged in the prefrontal cortex and cerebellum of male patients with cirrhosis and HE [15]. Despite the different conclusions of the above studies, these findings regarding MAO activity changes cannot explain the elevated brain 5-HT levels due to liver failure.

5-HT glucuronidation catalyzed by UDP-glucuronosyltransferases (UGTs), especially UGT1A6, is also an important catabolic pathway of this neurotransmitter [16–19]. Normally, UGT1A6 accounts for more than 50 % of 5-HT metabolism [18], increasing to 70 % when MAO activity is inhibited [16]. UGT1A6 is also highly expressed in the brain tissues of humans and rats [20,21] and is accompanied by high levels of brain 5-HT glucuronide conjugate (5-HT-G) [22,23], demonstrating the occurrence of 5-HT glucuronidation in the brain.

These results suggest that alterations in the activity and expression of UGT1A6 in the brain affect the regulation of 5-HT concentration in the brain and may contribute to neurological and psychiatric disorders. Expression of peripheral UGT1A6 is regulated by many factors such as hepatocyte nuclear factor 4α (HNF4α), NR-E2-related factor (Nrf2), aryl hydrocarbon receptor (AhR), and other stress-related factors [24,25]. The *Ugt1a6* promoter contains a xenobiotic response element domain responsible for AHR binding and HNF4 sites [26]. The expression of HNF4α mRNA is moderately correlated with that of UGT1A6 mRNA, inferring that HNF4α regulates hepatic UGT1A6 mRNA expression [27]. In caco-2 cells, UGT1A6 mRNA levels and glucuronide 5-HT activity were induced by both the AhR agonist TCDD and thymoquinone-induced oxidative stress [28]. Nrf2 is a key transcription factor that mediates oxidative stress responses [29] and its roles in regulating UGT1A6 have been demonstrated in Nrf2-knockout mice [30]. However, reports on UGT1A6 regulation have mainly focused on the periphery, and the regulatory mechanism of UGT1A6 in the brain remains unclear. The catalytic properties and expression of UGT1A6 in astrocytes are highly sensitive to redox environments [31,32]. HE is often associated with the accumulation of ammonia in the brain [33], and ammonia can affect neurons and astrocytes via oxidative stress [3,34,35]. This indicates that ammonia-mediated oxidative stress may also regulate brain UGT1A6 levels during liver failure.

To prove the above deductions and investigate the underlying mechanism, we used BDL rats as an animal model to simulate human cholestatic liver failure [36]. The aims of the present study were to: 1) investigate the associations between increased brain 5-HT concentrations and CNS behavioral abnormalities in BDL rats; 2) investigate whether BDL-induced liver failure alters UGT1A6 expression and activity to increase 5-HT content in the brain; and 3) identify the main factors affecting brain UGT1A6 expression and activity in the liver failure state and its mechanism using human astrocytes as an in vitro model. The results will reveal the mechanism by which BDL elevates brain 5-HT concentrations and elucidate its association with the behavioral abnormalities of HE.

2. Materials and methods

2.1. Reagents

All materials, antibodies, and primers used in this study are commercially available and listed in Tables S1, S2, and S3, respectively.

2.2. Animals

Male Sprague-Dawley (SD) rats were purchased from Sipul-Bicai Laboratory Animal Co. Ltd (Shanghai, China) and kept in controlled environmental conditions (12-h-light/dark cycle, temperature, 24 ± 2 °C; humidity, 50 % ± 5 %) with commercial rat chow and tap water available ad libitum. Animal experiments were conducted following the Guide for the Care and Use of Laboratory Animals (National Institutes of Health) and approved by the Ethics Committee of the Animal Care Committee of China Pharmaceutical University (protocol code No.

2019-06-016).

2.3. Development of BDL rats

Male SD rats (weighing 200–220 g) were used to establish BDL rats as previously described [9]. The sham-operated (SHAM) group was treated in the same manner without ligation of the bile duct. Fourteen days after surgery, six BDL and six SHAM rats were used for the open-field tests. Following the behavioral experiments, the rats were killed via femoral artery phlebotomy under isoflurane anesthesia. The blood and brain samples were quickly collected and stored at −80 °C until further analysis. Alanine transaminase (ALT), aspartate transaminase (AST), alkaline phosphatase (ALP), total bile acid, total bilirubin, and blood ammonia levels were measured using commercial kits (Table S1). The levels of 5-HT, DA, 5-hydroxy-L-tryptophan (5-HTP), 5-HIAA, and 5-HT-G in the serum and brain were measured using HPLC chromatography or LC-MS methods [9,23]. The MAO activity was measured using a previously described method [9]. Another six SHAM and six BDL rats were euthanized for mRNA, protein, and brain microsomal extractions.

2.4. Intracerebral injection of diclofenac sodium to rats

The intracerebroventricular (i.c.v.) injection experiments were conducted according to previous studies [37]. In brief, after 18 h of fasting, SD rats (weighing 180–200 g) were kept under isoflurane anesthesia and mounted in a David Kopf stereotaxic frame (Tujunga, CA, USA). A 22-gauge guide cannula (CMA12; CMA Microdialysis, Solna, Sweden) was implanted bilaterally in the left lateral ventricle of the brain (AP 0.8, V −3.0 from the dura and L −1.5 from the bregma) and secured to the skull with anchor screws and acrylic dental cement. After surgery, the animals were housed individually for four days.

At 5, 6, and 7 days after surgery, the rats were anesthetized as described above and placed in a stereotaxic apparatus for i.c.v. injections. Diclofenac sodium (4 mmol/L) or vehicle (artificial cerebrospinal fluid) were infused (5 μL in 5 min) by a CMA/100 micro infusion pump through a 28-gauge injection needle that was inserted through the guide and extended 1.0 mm beyond the tip of guide. The rats were subjected to open-field tests 4 h after the last diclofenac sodium injection or vehicle. After the behavioral experiments, the rats were euthanized as described above, and the left cortices of the rats were quickly collected for 5-HT and 5-HT-G level determination.

2.5. 5-HTP-treated rats

Twelve SD rats (weighing 180–200 g) were assigned to the 5-HTP and control (CON) groups. 5-HTP was dissolved in physiological saline (10 mg/mL) and administered via i.p. injection (100 mg/kg) once every 12 h for 72 h until the behavioral experiments were performed. CON rats received only physiological saline injections. The rats were subjected to behavioral experiments and then euthanized 2 h after the last dose. Brain samples were collected, and 5-HT levels were measured as we described in Section 2.3.

2.6. Hyperammonemic (HA) rats

HA rats were developed using i.p. NH_4Ac, as described in our previous study [33]. Twelve SD rats (weighing 180–200 g) were intraperitoneally administered NH_4Ac (3 mmol/kg) once every 12 h for 72 h as the HA group. The CON rats received only physiological saline injections (5 mL/kg). Six HA and six CON rats were subjected to behavioral experiments 2 h after the last dose and then euthanized as described above. The brain regions were collected for parameter determination and western blot analysis. Another Six HA and six CON rats were euthanized for cortical microsomal extraction.

2.7. Open-field tests

Open-field tests were performed as previously described [9]. Briefly, an open field was divided into inner and outer circles. Rats were individually placed at the center of an open-field apparatus and allowed to move freely for 5 min. The moving tracks were recorded using an open-field experimental video analysis system (Zhongshidichuang Institute, Beijing, China). Any-maze video tracking software was used to record and process the experimental data.

2.8. Brain microsome extraction

The experimental rats were decapitated, and whole brains or cortices were isolated for microsome extraction. Fresh brain tissues were homogenized in 0.05 mol/L tris-hydrochloride buffer (pH = 7.4), containing 0.15 mol/L KCl, 1 mmol/L ethylenediaminetetraacetic acid (EDTA), 1 mM dithiothreitol, and 0.1 mmol/L phenylmethylsulfonyl fluoride. Homogenates were centrifuged at 4 °C and 10000 g for 30 min. Then the supernatants were centrifuged at 100000×*g* for 60 min at 4 °C. Obtained microsomal pellets were suspended in the storage solution, consisting of 0.1 mol/L sodium phosphate buffer (pH = 7.4), 1 mmol/L EDTA, 1 mmol/L dithiothreitol, and 30 % (v/v) glycerol, aliquoted, and stored at −80 °C. The protein levels in the microsomes were measured using the BCA method.

2.9. Cell culture and drug treatment

U251 cells were purchased from the Chinese Academy of Medical Sciences (Shanghai, China) and cultured in Dulbecco's modified Eagle's medium (DMEM) containing 10 % fetal bovine serum. At 40 % confluence, the cells were incubated with DMEM containing 3 % fetal bovine serum and test agents for 72 h (the culture medium was replaced every 24 h) to assess the expression of target proteins and genes.

2.10. UGT1A6 activity determination

For UGT1A6 activity determination, U251 cells were seeded in 100 cm^2 culture dishes at 30 % density. After incubation with tested agents for 72 h, the cells were digested by trypsin and then collected and resuspended in 200 μL phosphate-buffered saline. The cell suspension was disrupted using ultrasound in an ice water bath and stored at −80 °C. The protein content was measured using the BCA method.

We chose 4-nitrophenol and 5-HT as substrates to determine UGT1A6 activity. The reaction was run in substrates, 10 mmol/L $MgCl_2$, 0.1 mol/L Tris-HCl buffer, 80 μg/mL Triton-X 100, 5 mM D-(+)-Dextronic acid δ-lactone, 5 mM UDPGA, pH 7.4 in the presence of 0.5 mg protein/mL brain microsomes or cell lysates at 37 °C. After 2 h of incubation, 100 μL ice acetonitrile with 0.2 % formic acid was added to terminate the reaction. The 4-nitrophenyl β-D-glucuronide (PNPG) and 5-HT-G concentrations in the reaction systems were measured using high-performance liquid chromatographic methods above described.

2.11. Immunofluorescence assay

All antibodies used in the immunofluorescence assays are listed in Table S2. Immunofluorescence assays of the brain sections were conducted as we previously described [38]. Briefly, after deparaffinization, paraffin-embedded sections of rat brains were incubated with normal goat serum and mixed with primary antibodies against mouse anti-UGT1A6 and rat anti-GFAP. The sections were then incubated with anti-rabbit IgG (Alexa Fluor 488-conjugated) and anti-mouse IgG (Alexa Fluor 594-conjugated) secondary antibodies. Finally, immunofluorescence images of brain sections were obtained using confocal laser scanning microscope (Zeiss LSM700).

The U251 cells were incubated with 5 mM NH_4Cl. After 72 h incubation, the cells were fixed with 4 % formaldehyde for 15 min and then

blocked with 5 % goat serum in PBS at 25 °C. Cells were incubated overnight with primary antibodies against mouse anti-UGT1A6. After washing with PBS, the U251 cells were incubated with Alexa Fluor 488-conjugated anti-rabbit IgG for 1 h at 25 °C. Nuclei were stained with 4',6-diamidino-2-phenylindole. Immunofluorescence images of U251 cells were obtained using a Cytation 5 Cell Imaging Multi-Mode Reader (BioTek, Germany) and processed using Gen 5 software (BioTek, Germany).

2.12. In vitro transfection

Human HNF4α siRNA (5'–3' sense: CCUAGGCAAUGACUACAUUTT) was validated in our previous study [39] and synthesized by GenePharma (Shanghai, China). For HNF4α knockdown, U251 cells were transfected with 100 nM siRNA using Lipofectamine 3000 according to the manufacturer's instructions. The cells were subjected to drug treatment 12 h after transfection, and the silencing efficiency was verified by western blotting 72 h post-transfection. Scrambled siRNA was used as the negative control.

2.13. Dual luciferase assay

The PGL3-H_Ugt1a6 promoter-luciferase reporter and pCDNA3.1-based HNF4α expression plasmid were constructed by Jiangsu KeyGEN Biotech Co., Ltd. (Nanjing, China). The NIH/3T3 cells were purchased from Cellcook Biotech (Guangzhou, China). NIH/3T3 cells were transfected with PGL3-H_Ugt1a6 promoter luciferase reporter (0.2 mg/well) and Hnf4α plasmid (0, 50, 100, 200 ng/well) using Lip3000 and P3000 12 h after seeding in 24-well plates. The NIH/3T3 cells were lysed 48 h post-transfection. The luciferase activity was measured using a luciferase assay kit (Yeasen, Shanghai, China).

U251 cells were also transfected with PGL3-H_Ugt1a6 promoter-luciferase reporter together with the HNF4α siRNA, HNF4α plasmid, or treated with 5 mmol/L NH_4Cl or 1 μmol/L U0126. The luciferase activity was measured 72 h after transfecting the U251 cells.

2.14. qPCR

The total mRNA was extracted from tissues and cells and reverse transcribed into cDNA as previously described [40]. qPCR amplification was performed using the qPCR SYBR Green Master Mix (Yeasen, Shanghai) and the corresponding primers (Table S3) on a LightCycler 96 Real-Time PCR System (Roche Applied Science, Indianapolis, IN, USA). The relative mRNA levels were normalized to those of ACTB using the comparative Ct method.

2.15. Western blot

The total protein was extracted from tissues and cells and separated via sodium dodecyl sulfate-polyacrylamide gel electrophoresis and transferred onto nitrocellulose membranes. Following 1.5 h of blocking at 25 °C, the blots were incubated with corresponding primary antibodies (Table S2) at 4 °C overnight. After washing thrice with TBST, the blots were incubated with secondary antibodies for 1 h at room temperature. The protein levels were visualized using ECL kits (Jiangsu keyGEN BioTECH Co., Ltd., Nanjing), followed by a gel imaging system (Tanon Science & Technology Co. Ltd., Shanghai), and normalized to β-Actin levels.

2.16. Statistical analysis

Data were analyzed using GraphPad Prism version 8.0.2. $P < 0.05$ indicated statistical significance. All data in the experiment are presented as mean ± SEM, and comparisons between two groups were statistically tested using an unpaired two-tailed Student's T-Test; one- or two-way ANOVA, followed by Fisher's LSD multiple comparison tests, were used for comparisons among multiple groups.

3. Results

3.1. BDL rats showed behavioral abnormalities and higher brain 5-HT levels

BDL surgery was performed on rats to induce cholestatic liver failure. Fourteen days after surgery, we evaluated the physiological and biochemical parameters of the BDL and SHAM rats (Table S4). The results demonstrated that BDL rats showed significantly higher levels of serum ALT, AST, ALP, total bile acids, total bilirubin, blood ammonia, and increased liver and spleen weights compared with those in SHAM rats, which proved the successful development of the BDL-induced liver failure model.

The open-field test was used to examine the behavioral changes in BDL rats. The results showed that BDL significantly increased both the total and inside traveled distance and increased the percentage of time spent in the center and climbing times (Fig. 1A–E). The concentrations of 5-HT and DA in the brain and plasma of rats were measured. The results demonstrated that BDL significantly increased the levels of DA and 5-HT in the rat cerebral cortex (but not in the hippocampus) (Fig. 1F and G). The levels of cortical 5-HT in BDL rats were nearly 2-fold higher than those in SHAM rats (Fig. 1F), and BDL had little effect on the levels of plasma DA and 5-HT (Fig. 1H).

3.2. BDL decreased UGT1A6 expression and activity to elevate 5-HT levels in cortices of rats

The levels of 5-HT in the plasma of the BDL rats were unaltered (Fig. 1H), indicating that the increased cortical 5-HT levels induced by BDL were mainly attributed to alterations in the synthesis and metabolism of 5-HT in the brain. BDL had little effect on the mRNA expression of *Tph2* in the hippocampus and cortex, as well as on TPH2 protein expression in the hippocampus, but significantly reduced the expression of TPH2 protein in the rat cortex (Fig. 2A and B). The levels of 5-HTP, the direct product catalyzed by TPH2 and the prodrug 5-HT, were unaltered in BDL rats (Fig. 2C). Moreover, BDL had little effect on the expression levels and activities of MAO-A and MAO-B in the rats (Fig. 2D–G), consistent with the lack of alterations in the levels of 5-HIAA (Fig. 2H). These results suggest that BDL increases brain 5-HT concentrations independently of the classical 5-HT synthetic or metabolic pathways.

The glucuronidation of 5-HT catalyzed by UGT1A6 is also an important catabolic pathway of this neurotransmitter [16–19]. Remarkably decreased cortical 5-HT-G content was detected in BDL rats, which decreased from 73.09 ± 11.52 ng/g in SHAM rats to 34.81 ± 5.84 ng/g in BDL rats (Fig. 2I). The ratio of 5-HT-G to 5-HT content also significantly decreased in the cortex of BDL rats (Fig. 2J), in line with the downregulation of cortical UGT1A6 mRNA and protein expression in BDL rats (Fig. 2K and L). The activity of UGT1A6 in the brain microsomes was also measured. The formation rate of PNPG from 4-nitrophenol and 5-HT-G from 5-HT in brain microsomes of BDL rats was significantly decreased (Fig. 2M and N). These results indicate that BDL elevated 5-HT levels in the cortex of rats due to the downregulation of cortical UGT1A6 expression and activity.

3.3. Effects of i.c.v. UGT1A6 inhibitor diclofenac on cortical 5-HT levels

To verify whether the downregulation of cerebral UGT1A6 contributed to the increased levels of 5-HT in the rat cortex, diclofenac sodium was administered via i.c.v. injection into the experimental rats (DIC rats) (Fig. 3A). The cortical UGT1A6 activities and 5-HT levels were measured 4 h after the last injection. The results showed that i.c.v. diclofenac concentration-dependently decreased PNPG formation rate in the brain microsomes of DIC rats (Fig. 3B). Diclofenac injection also significantly increased 5-HT levels (Fig. 3C) while decreasing 5-HT-G levels in the

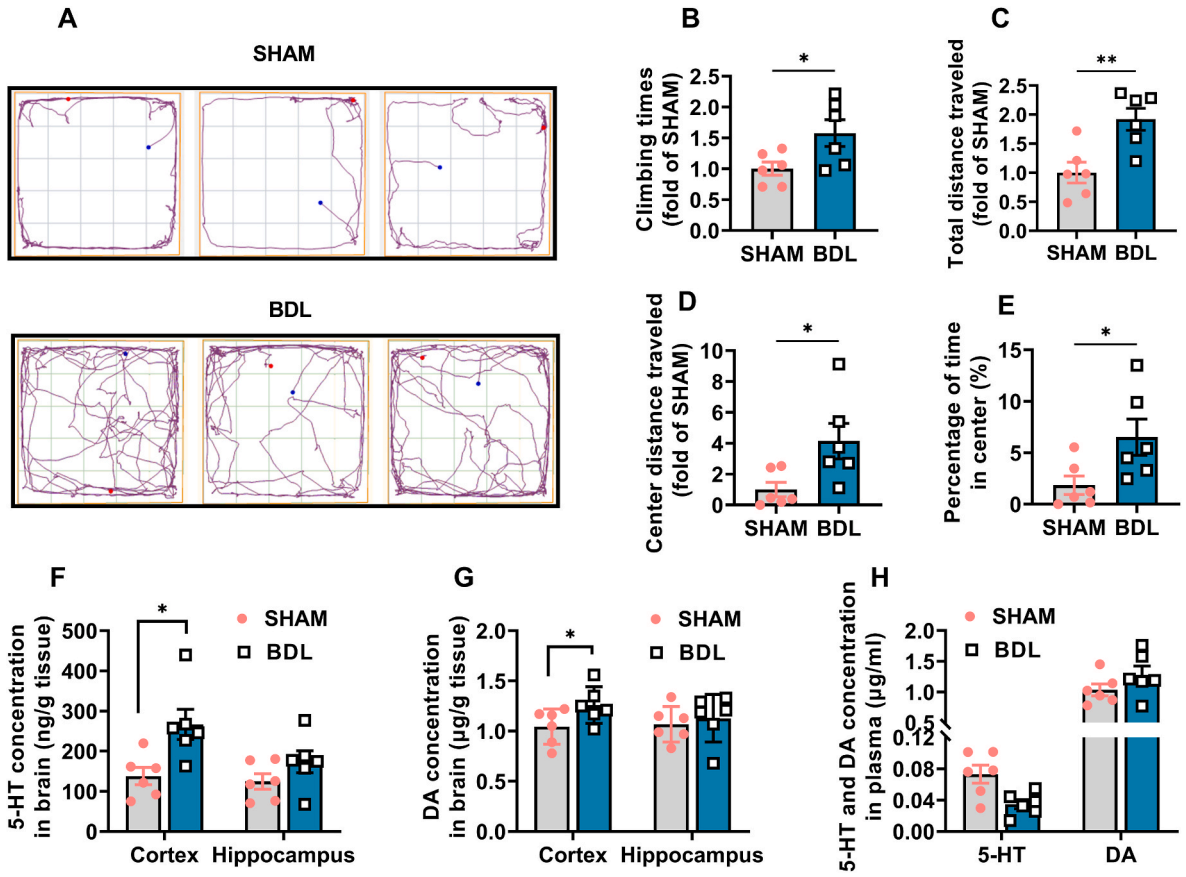

Fig. 1. BDL rats showed behavioral abnormalities and higher brain 5-HT levels. Track diagram (A), climbing times (B), total distance traveled (C), inside distance traveled (D), and percentage of time in center (E) of bile duct ligation (BDL) and SHAM rats in open-field test. Concentrations of 5-HT (F) and DA (G) in cortex and hippocampus of BDL and SHAM rats. Concentrations of 5-HT and DA in the plasma of BDL and SHAM rats (H). Data are expressed as mean ± SEM (n = 6), $^{*}P < 0.05$, $^{**}P < 0.01$.

cortex of rats (Fig. 3D). Moreover, similar to the BDL rats, the DIC rats also showed an increased inside traveled distance in the open-field test (Fig. 3H), Other parameters such as total traveled distance and climbing times also increased, but no significant differences were observed due to individual difference (Fig. 3E–I).

3.4. 5-HTP treatment induced HE-like behaviors

The synthesis of 5-HT from tryptophan proceeds via intermediary 5-HTP, which easily crosses the BBB. To examine the role of increased cortical 5-HT levels in the behavioral abnormalities in BDL and DIC rats further, 5-HTP (100 mg/kg) was intraperitoneally injected into the experimental rats (Fig. 4A). This is consistent with our expectation that 5-HTP treatment would significantly elevate cerebral 5-HT levels in rats (Fig. 4B). More importantly, 5-HTP rats showed similar behavioral changes to BDL and DIC rats, such as an increased total and inside distance traveled, percentage of time spent in the center and climbing times in the open field test (Fig. 4C–G). These results proved the contribution of cortical 5-HT overload to HE-like symptoms.

3.5. BDL-induced ammonia accumulation impaired cortical UGT1A6 activity and expression

The present study demonstrated that UGT1A6 and glial fibrillary acidic protein (GFAP, a characteristic astrocyte protein) were co-expressed in the rat cortex (Fig. S1A). In addition, U251 cells (astrocytes) had the highest UGT1A6 mRNA expression (Fig. S1B) and activity (Figs. S1C and D) compared with brain microvascular endothelial cells (HCMEC/D3) and neurocytes (SH-SY5Y). Thus, U251 cells were chosen as the in vitro model to investigate the mechanism of the BDL-mediated decrease in UGT1A6 expression and activity.

Cholestasis is often associated with abnormal increases in bilirubin, ammonia, bile acids, and inflammatory cytokines levels. We investigated whether these changes reduced UGT1A6 expression in U251 cells. The results demonstrated that only NH_4Cl significantly downregulated *UGT1A6* mRNA expression (Fig. 5A), whilst both 50 μM unconjugated bilirubin (UCB) and 5 mM NH_4Cl decreased UGT1A6 activity, and NH_4Cl inhibited UGT1A6 activity more strongly than UCB (Fig. 5B). Further studies showed that the inhibitory effects of UCB on UGT1A6 activity were not concentration-dependent (Fig. 5C) and UCB slightly influenced *UGT1A6* mRNA expression (Fig. 5D). In contrast, NH_4Cl concentration-dependently decreased UGT1A6 activity (Fig. 5E), as well as its mRNA (Fig. 5F), and protein levels (Fig. 5G). Under 5 mM NH_4Cl treatment, UGT1A6 protein levels were significantly downregulated to approximately 50 % of those in the CON group (Fig. 5G–I). These results indicate that the downregulation of UGT1A6 activity and expression is mainly attributable to brain ammonia accumulation.

3.6. Ammonia-induced oxidative stress decreased expression and activity of UGT1A6 by activating ROS-ERK pathway

Ammonia can activate signaling pathways such as NF-kB, PI3K-AKT, and ERK [33,41,42]. To investigate the mechanism of ammonia-mediated reduction in UGT1A6 expression and activity, U251 cells were incubated with NH_4Cl and different signaling pathway blockers, BAY117082, LY294002, and U0126 (Fig. 6A–C). The results showed that only U0126, an ERK pathway inhibitor, could reverse the reduction in UGT1A6 activity by NH_4Cl (Fig. 6C). Activation of the ERK

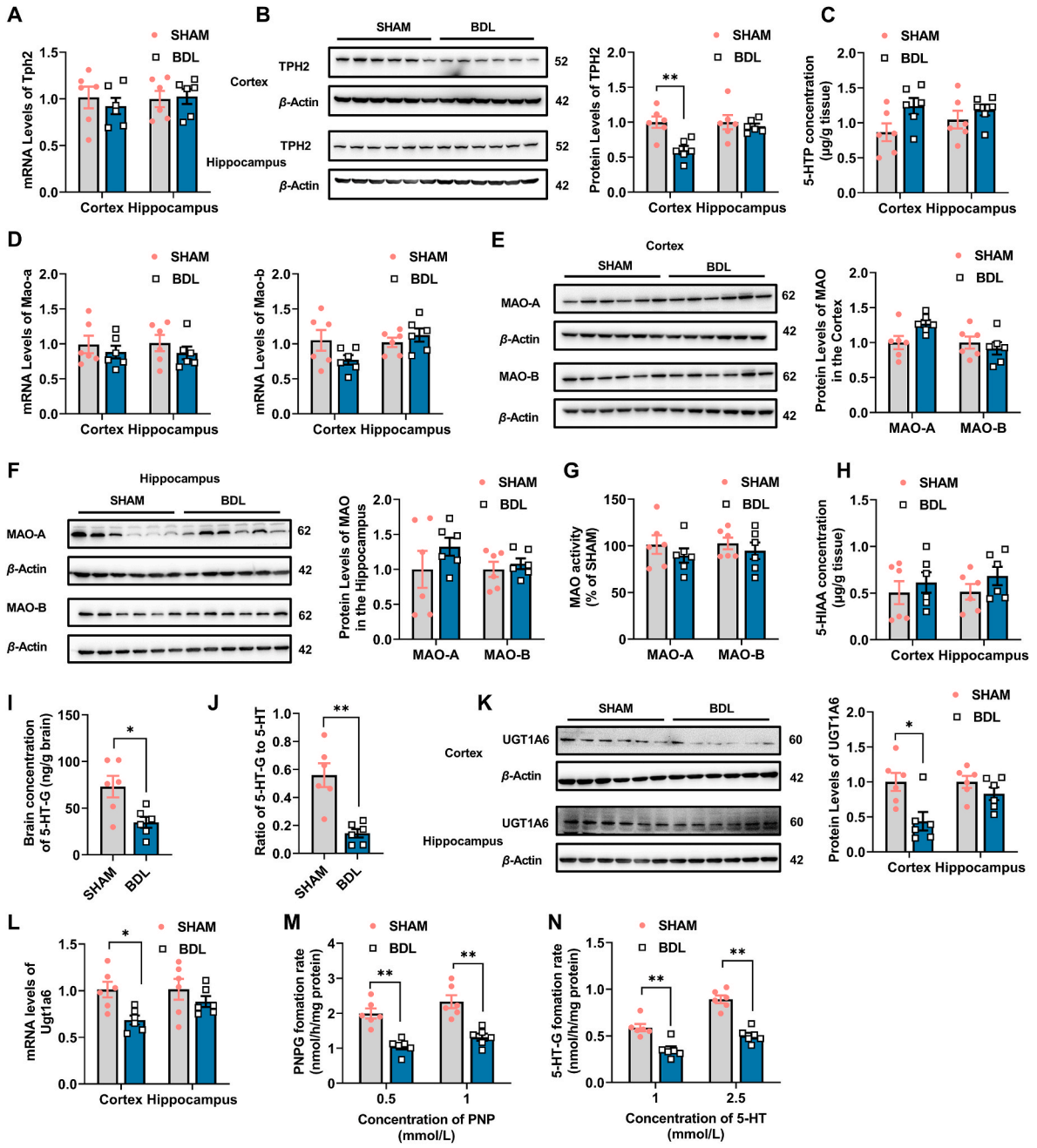

Fig. 2. BDL decreased UGT1A6 expression to elevate cortical 5-HT levels. mRNA (A) and protein (B) levels of TPH2, and concentrations of 5-HTP (C) in cortex and hippocampus of BDL and SHAM rats. mRNA (D) and protein (E and F) levels and activities (G) of MAO-A and MAO-B, and concentrations of 5-hydroxyindole-acetic acid (5-HIAA) (H) in cortex and hippocampus of BDL and SHAM rats. Concentrations of 5-HT glucuronide conjugate (5-HT-G) (I) and the ratio of 5-HT-G to 5-HT (J) in cortex of BDL and SHAM rats. Protein (K) and mRNA (L) levels of UGT1A6 in cortex and hippocampus of BDL and SHAM rats. Formation rate of 4-Nitrophenyl β-D-glucuronide (PNPG) (M) and 5-HT-G (N) for microsomes of BDL and SHAM rats. Data are expressed as mean ± SEM (n = 6) *$P < 0.05$, **$P < 0.01$.

pathway is often associated with oxidative stress, which ammonia can induce in the brain [33]. In line with this, 72 h of NH_4Cl treatment significantly increased reactive oxygen species (ROS) levels (Fig. 6D) and p-EKR protein expression (Fig. 6E) in U251 cells while reducing UGT1A6 protein expression (Fig. 6E).

H_2O_2 showed effects similar to those of NH_4Cl (Fig. 6F–H), and the increase in ROS levels and downregulation of UGT1A6 activity by NH_4Cl or H_2O_2 was reversible using the antioxidant N-acetyl-L-cysteine (NAC) (Fig. 6F and H). In addition, the effects of NH_4Cl on UGT1A6 and p-ERK expression could also be reversed by NAC (Fig. 6I) or the ERK pathway inhibitor U0126 (Fig. 6J). These results demonstrate that ammonia impairs the expression and activity of UGT1A6 by activating the oxidative stress-mediated ROS-ERK pathway in U251 cells.

Similar results were observed in the cortex of BDL rats. BDL significantly increased ROS levels (Fig. 6K) and reduced SOD activity (Fig. 6L) in the cortex, accompanied by the induction of ERK phosphorylation and downregulation of UGT1A6 protein levels (Fig. 6M). Relationship analysis showed that UGT1A6 protein levels in the cortex of BDL and SHAM rats were negatively correlated with the ratio of pERK to ERK ($R = -0.72$, $P < 0.01$) (Fig. 6N).

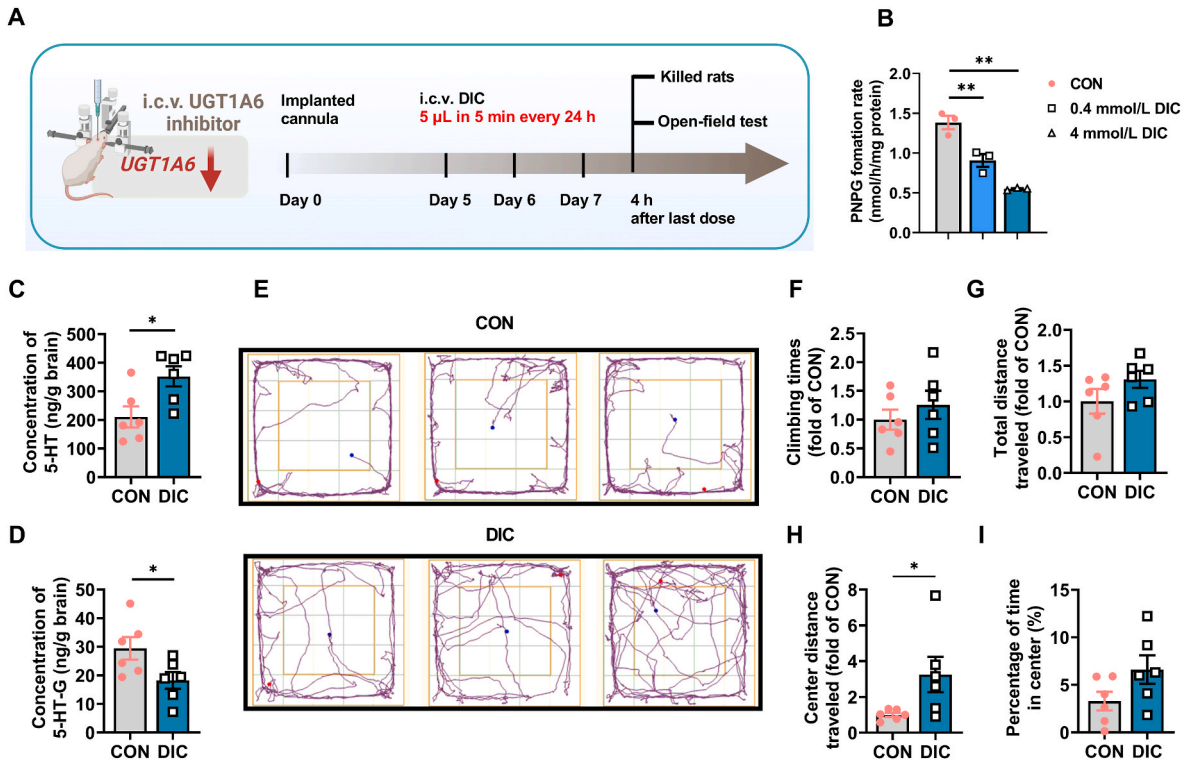

Fig. 3. UGT1A6 declination elevated cortical 5-HT levels in rats. Schematic diagram of the experiment (A). Effects of i.c.v. diclofenac sodium (DIC) on PNPG formation rate in brain microsome of rats (B). Concentrations of 5-HT (C) and 5-HT-G (D) in cortex of DIC and CON rats. Track diagram (E), climbing times (F), total distance traveled (G), center distance traveled (H), and the percentage of time in center (I) of DIC and CON rats in the open-field test. Data are expressed as mean ± SEM (n = 3 for B, n = 6 for C–I), $^{*}P < 0.05$, $^{**}P < 0.01$.

3.7. ROS-ERK pathway activation inhibited HNF4α expression to decrease UGT1A6 transcription

HNF4α is involved in the inter-individual variability of UGT1A6 mRNA expression in humans [27]. Inhibition of the ERK phosphorylation increases the expression of HNF4α mRNA and protein [43]. These results indicated that the downregulation of UGT1A6 via ammonia may be involved in the inhibition of HNF4α. To test this hypothesis, U251 cells were cultured with NH_4Cl or the ERK activator, TBHQ. The results showed that both NH_4Cl and TBHQ significantly downregulated the expression of HNF4α protein (Fig. 7A), and U0126 remarkably reversed the downregulation of HNF4α expression by NH_4Cl (Fig. 7B), demonstrating that NH_4Cl inhibited HNF4α protein expression via activating the ERK pathway.

The roles of HNF4α in regulating UGT1A6 expression were further investigated, and the results demonstrated that both TBHQ treatment and HNF4α silencing significantly decreased UGT1A6 protein expression (Fig. 7C and D). To investigate whether HNF4α directly activates the promotor of *Ugt1a6*, different doses of the Hnf4α plasmid (50, 100, and 200 ng) and PGL4.10-M_Ugt1a6 promoter-luciferase reporter constructs were co-transfected into NIH/3T3 cells. The results showed that the Hnf4α plasmid dose-dependently increased the luciferase activity of the *Ugt1a6* promoter (Fig. 7E). U251 cells were also transfected with the PGL4.10-M_Ugt1a6 promoter-luciferase reporter construct. Both NH_4Cl treatment and the silencing of HNF4α significantly suppressed *Ugt1a6* promoter activity (Fig. 7F). Further studies showed that both the Hnf4α plasmid and U0126 reversed the decrease in *Ugt1a6* promoter activity induced by NH_4Cl (Fig. 7F). Significantly decreased expression of HNF4α was also detected in the cortex of BDL rats (Fig. 7G). These results indicate that ammonia downregulates UGT1A6 expression by inhibiting HNF4α expression via activating the ROS-ERK pathway.

3.8. Hyperammonemia increased 5-HT content and lowered UGT1A6 activity and expression in cortices of rats

Hyperammonemia (HA) rats were developed to demonstrate further the role of ammonia in downregulating UGT1A6 expression and elevating 5-HT content in rat cortices. The findings were similar to those in BDL rats that HA significantly lowered the expression and activity of UGT1A6 protein (Fig. 8A and B) in the cortex of rats, accompanied by remarkably increased levels of cortex 5-HT (Fig. 8C). The open-field test also showed that HA rats exhibited increased total travel distance, center travel distance, and climbing times (Fig. 8D–H).

HA rats also showed significantly elevated cortical ROS levels (Fig. 8I) and decreased SOD activity (Fig. 8J), demonstrating the occurrence of oxidative stress in the cortex of HA rats. Consequently, significantly increased ERK phosphorylation and decreased protein levels of HNF4α were observed in the cortex of HA rats (Fig. 8K), resulting in reduced cortical UGT1A6 expression and activity.

4. Discussion

HE is a commonly encountered neurocognitive complication in chronic and acute liver diseases, and its typical symptoms include mania, anxiety, depression, and other cognitive and behavioral abnormalities. The present study systematically demonstrated that BDL-induced manic-like behaviors are partly due to cerebral UGT1A6-expression-and-activity-reduction-mediated CNS 5-HT overload caused by activating the ammonia-mediated ROS-ERK-HNF4α pathway. To the best of our knowledge, this is the first report to reveal the mechanism involving elevated brain 5-HT concentration in rats with BDL-induced liver failure and its association with cognitive and behavioral abnormalities in HE.

Clinical trials and animal experiments have demonstrated that HE is often associated with the accumulation of neurotransmitters in the

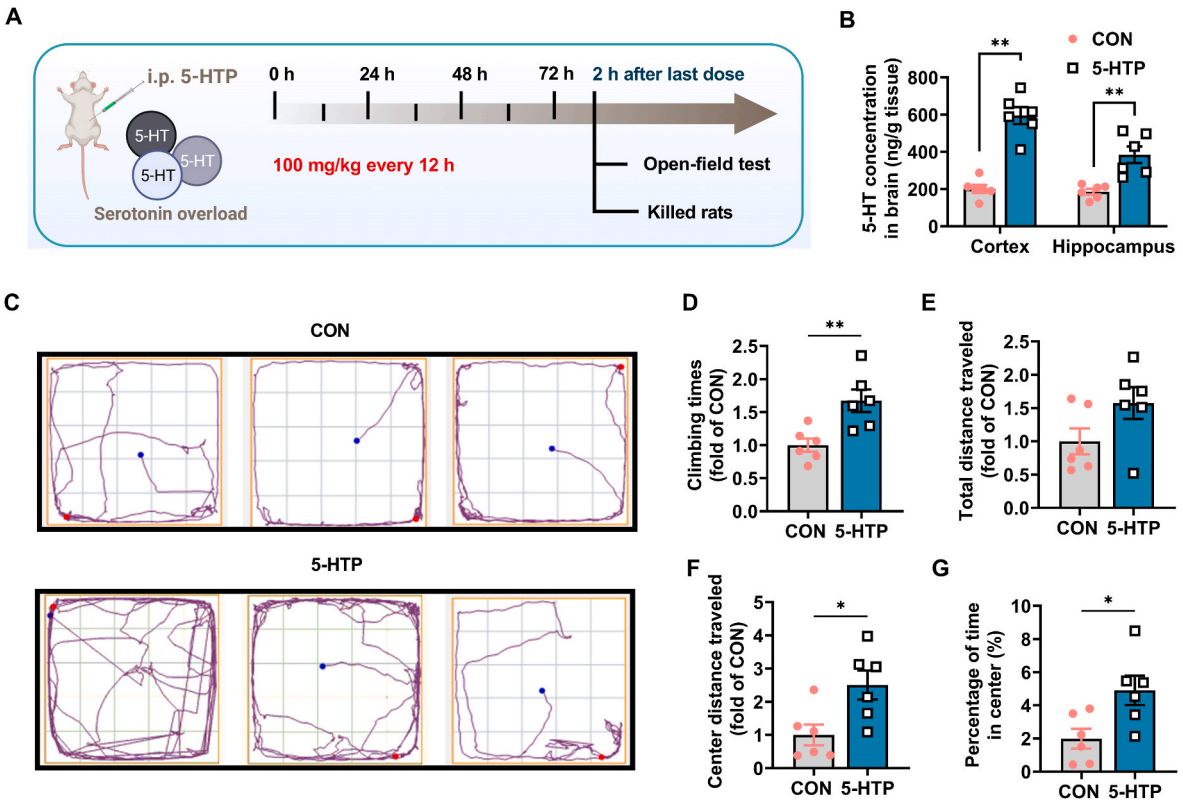

Fig. 4. 5-HTP treatment induced HE-like behaviors. Schematic diagram of the experiment (A). Concentrations of 5-HT in the cortex and hippocampus of CON (rats treated with saline) and 5-HTP rats (rats treated with 100 mg/kg 5-Hydroxytryptophan) (B). Track diagram (C), climbing times (D), total distance traveled (E), center distance traveled (F), and the percentage of time in center (G) of CON and 5-HTP rats in the open-field test. Data are expressed as mean ± SEM (n = 6) $^{*}P < 0.05$, $^{**}P < 0.01$.

brain. Significantly increased levels of DA, histamine, gamma-aminobutyric acid, and 5-HT were detected in the cerebrospinal fluid of patients with HE [8], and significantly increased levels of 5-HT were also detected in the cortex of TAA-induced HE rats [44]. Our previous study revealed that BDL increases cerebral DA levels by upregulating tyrosine hydroxylase expression [9]. The present study further revealed that BDL significantly increased both 5-HT and DA levels in the rat cortex, and the extent of the increase in 5-HT was greater than that of DA. Dyshomeostasis of brain 5-HT concentration is involved in numerous CNS diseases [11], with symptoms similar to HE [45]. The present study demonstrated that BDL rats showed typical manic-like behaviors in the open-field tests, which is in line with findings in other research [9]. However, a recent study demonstrated that BDL mice showed locomotor impairment in open-field tests [46]. These different findings may come from differences in the degree of liver damage. It is worth noting that manic-like behaviors were also observed in rats with cerebral 5-HT overload caused by 5-HTP treatment. 5-HTP has been widely used to manipulate cerebral 5-HT levels; in rodents, 200–300 mg/kg 5-HTP can induce memory impairment, confusion, and anxiety [47,48]. These studies suggest that cerebral 5-HT overload may be one of the causes of behavioral abnormalities in HE.

Besides the cortex and hippocampus, the homeostasis of 5-HT in other brain regions like the striatum and raphe nucleus also plays an important role in behavior regulation [49,50]. Decreases in striatal 5-HT levels are involved in suppressed locomotor activity in mice [50], and the raphe nucleus constitutes a major serotonergic input to the forebrain and modulates diverse functions and brain states, including anxiety and motor functions [49]. Our results showed that BDL-induced liver failure little influenced striatal 5-HT levels (Fig. S2A) and the mRNA levels of enzymes (Tph2, Mao-a, Mao-b, and Ugt1a6) related to 5-HT metabolism and synthesis (Fig. S2B). We also found that BDL unaltered DA levels in the striatum of BDL rats (Fig. S2C). Similar results were also found both in patients with HE and TAA-induced HE rats: In TAA rats, DA and 5-HT levels were significantly increased in the cortex but not in the striatum, and the extent of these changes in the cortex correlated with the stage of HE [44]. Increased 5-HT levels were found in the cerebrospinal fluid and frontal cortex of patients with HE [8,51]. Thus, the present study focused on the cortex, and the important roles of the striatum-putamen complex and raphe nucleus in the HE state still need further exploration.

Due to the presence of the BBB, the synthesis and metabolism of 5-HT in the CNS are relatively independent [11]. Our results demonstrated that BDL had no significant influence on the expression and activity of TPH2 and MAO or on their metabolite concentrations in the cortex of rats, which excludes the roles of the classical 5-HT synthetic or metabolic pathways in BDL-induced cerebral 5-HT overload. UGT1A6-catalyzed glucuronidation is also important for 5-HT metabolism [16–19]. We verified the existence of UGT1A6 expression and its activity in the rat brain and found that BDL-induced liver failure significantly decreased the expression and activity of UGT1A6 and the levels of 5-HT-G in the cortex of rats. Serotonin transporter (SERT) is also essential for serotonergic system regulation. However, unlike serotonin-related metabolic enzymes (TPH2, MAO, and UGT1A6), SERT tends to regulate the concentration of 5-HT in the synaptic cleft rather than the total concentration of 5-HT in the brain tissue, and the predominance of SERT sites in substantia nigra, raphe nucleus, striatum, and thalamus [52,53]. Ischemia-induced liver injury has been shown to downregulate SERT activity in the cortex and striatum, and in the frontal cortex, this loss of SERT function was accompanied by increases of 5-HT concentrations in extracellular fluid (from 13.2 to 14.1 pg/20 mL) [54]. We also found a slight decrease in *Sert* mRNA expression (23 % reduction) in the cortex but not in the hippocampus and striatum of BDL rats (Fig. S2D), but due to experimental limitations, we did not measure

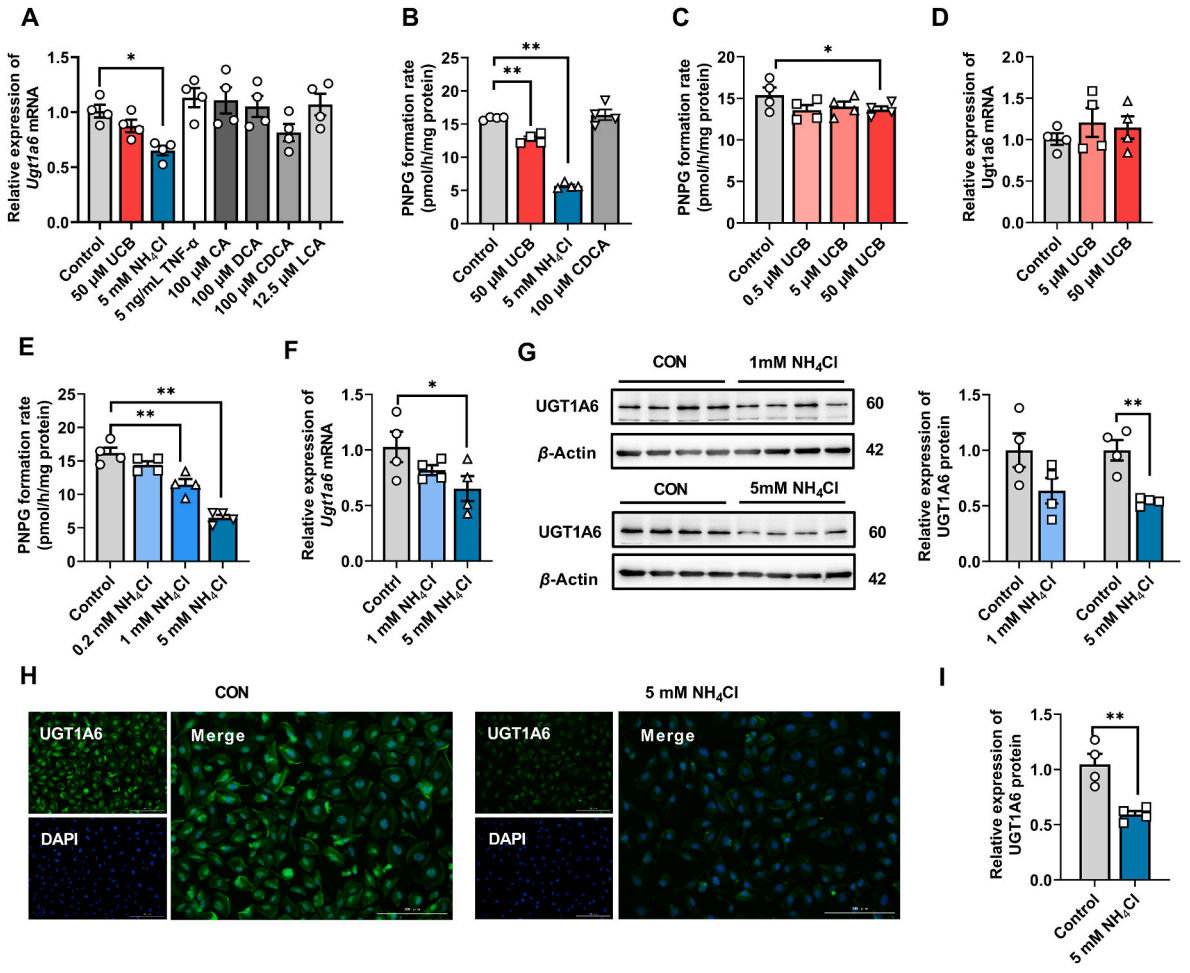

Fig. 5. Ammonia decreased the activity and expression of UGT1A6 in U251 cells. UGT1A6 mRNA levels (A) and activity (B) changes in U251 cells under the treatment of unconjugated bilirubin (UCB), NH_4Cl, TNF-a, and bile acids. PNPG formation rate and UGT1A6 mRNA levels in U251 cells under the treatment of concentration-elevated UCB (C and D) or NH_4Cl (E and F). Western bolting (G) and immunofluorescence (H and I) experiment demonstrated changes in UGT1A6 protein levels in U251 cells treated with NH_4Cl. Data are expressed as mean ± SEM (n = 4) $^*P < 0.05$, $^{**}P < 0.01$.

5-HT levels in extracellular fluid of BDL rats, which is one of limitation of the present study. Whether BDL-induced SERT expression changes could synergize decreased UGT1A6 expression in the cortex to affect rat behavior is also worthy of further exploration. The main findings of our study were an increase in the total content of 5-HT and a decrease in 5-HT-G in the rat cortex, and we found that i.c.v. injection of the UGT1A6 inhibitor, diclofenac sodium, significantly increased cerebral 5-HT levels, leading to HE-like behaviors in rats. These results indicate that BDL mainly decreases the expression and activity of UGT1A6 to elevate 5-HT levels in the rat cortex, contributing to neurological and psychiatric disorders in HE.

In the mammalian brain, the ability to synthesize and release 5-HT is a property shared by less than 0.1 % of neurons [55,56], and the specific activity of UGT1A6 in astrocytes is 10- and 100-fold those of neurons or total brain [57]. Our results also showed that UGT1A6 is mainly expressed in brain astrocytes; therefore, U251 cells were used as an in vitro model for further mechanistic studies. Ammonia could reduce the expression and activity of UGT1A6 in U251 cells in a concentration-dependent manner. As BDL-induced liver failure is often accompanied by hyperammonemia, we were not surprised by these results. The local ammonia concentration in the brain can reach mMOL levels in the HE state [58]. Ammonia diffuses rapidly throughout the brain, but ammonia poisoning mainly occurs in the endothelial cells and astrocytes of the BBB [59,60]. The distribution and response of astrocytes are region-specific in the brain [61], which leads to different sensitivities to stress among brain regions [62–65]. Ammonia-induced oxidative stress primarily occurs in the cortex rather than in the striatum [64], which explains why we found that ammonia has the most significant effect on loss of UGT1A6 expression and increases in 5-HT concentration in the cortex of BDL rats. It was reported that the cortex is sensitive to ischemic stress, while the striatum and thalamus are not [63]. Similarly, cerebral artery ischemia-reperfusion- or iron overload-induced oxidative stress mainly occurs in the cortex [62,65]. These studies also support our findings.

Ammonia accumulation can activate multiple signaling pathways in the brain. Our study demonstrated that ammonia-mediated brain UGT1A6 expression and activity reduction are mainly related to the activation of the ROS-ERK pathway mediated by oxidative stress. In U251 cells, we found both NH_4Cl and H_2O_2 significantly increased ROS levels and induced ERK phosphorylation while decreasing UGT1A6 expression and activity; these effects of NH_4Cl could be reversed by antioxidant NAC or ERK inhibitor U0126. Recent studies have also partly confirmed our findings: oxidative stress-induced ERK activation has been found in a variety of cell types [66–68], hyperammonemia can show its effect on astrocytes by inducing oxidative stress [34,35,69], and the catalytic properties and expression of UGT1A6 in astrocytes are highly sensitive to the redox environment [31,32]; Our previous studies have also demonstrated that ammonia-induced oxidative stress can activate the ROS-ERK pathway to regulate breast cancer resistance protein expression in the brains of rats with acute liver failure [33].

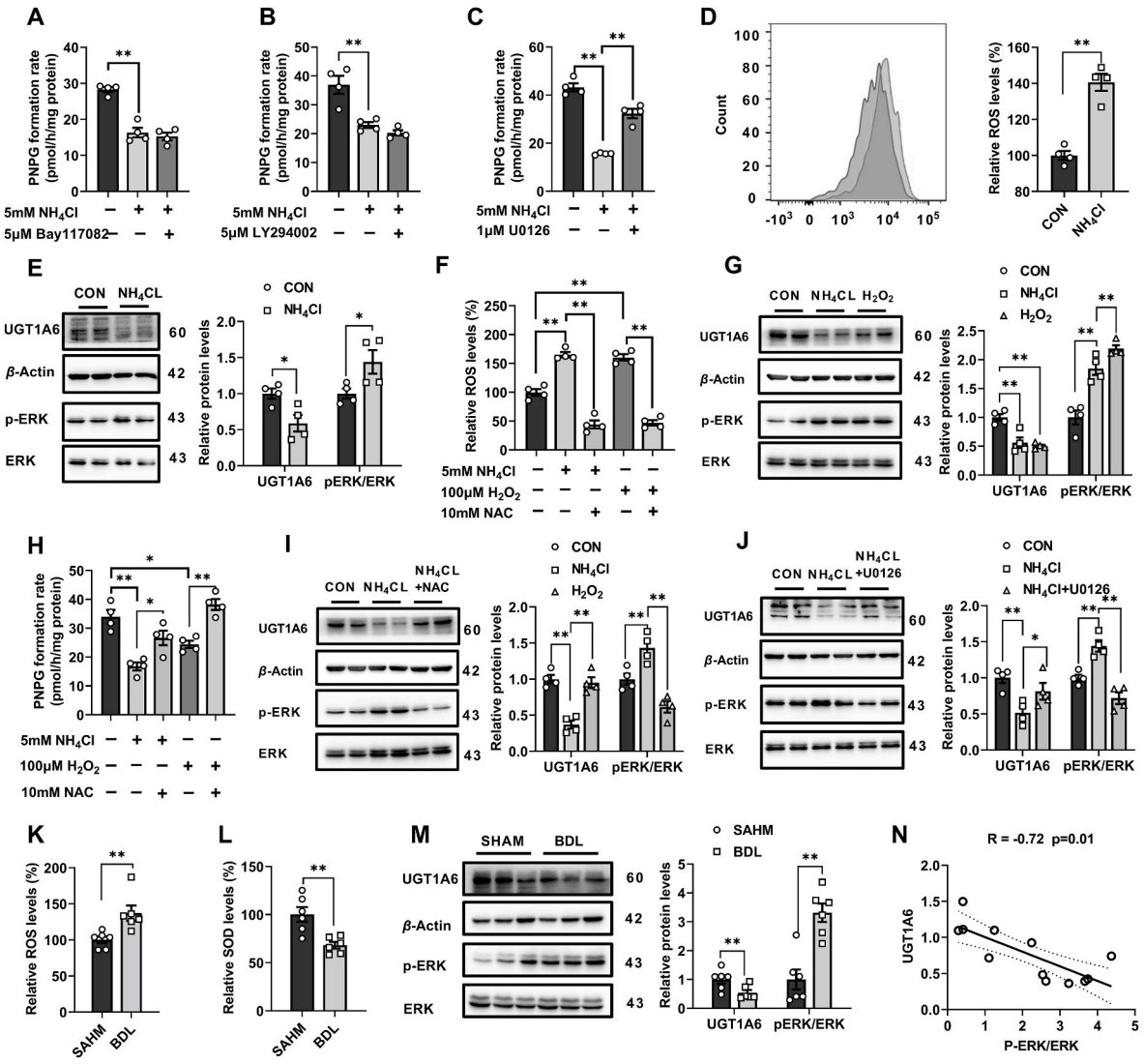

Fig. 6. Possible mechanism of ammonia-mediated reduction in UGT1A6 expression and activity. Activities of UGT1A6 in U251 cells following treatment with NH_4Cl and different signaling pathway blockers BAY117082 (A), LY294002 (B), and U0126 (C). Effects of NH_4Cl on reactive oxygen species (ROS) levels (D) and protein levels of UGT1A6 and p-ERK (E). Effects of NH_4Cl, H_2O_2, and N-acetyl-L-cysteine (NAC) on ROS levels (F) and UGT1A6 activity (H) in U251 cells. Effects of NH_4Cl and H_2O_2 on UGT1A6 and p-ERK protein levels in U251 cells (G). Effects of NAC (I) and U0126 (J) on NH_4Cl-mediated decrease in UGT1A6 levels and induction in p-ERK in U251 cells. Relative ROS (K) and SOD levels (L), and UGT1A6 and p-ERK protein levels (M) in the cortex of BDL and SHAM rats. Correlative analysis between UGT1A6 protein levels and the ratio of p-ERK/ERK in BDL and SHAM rats (N). Data are expressed as mean ± SEM (n = 4 for data on U251 cells, n = 6 for data on BDL and SHAM rats). $^*P < 0.05$, $^{**}P < 0.01$.

The expression of UGT1A6 can also be controlled by many environmental factors through stress-mediating receptors. Valproic acid treatment significantly induces UGT1A6 mRNA expression in Caco-2 cells via the AhR and Nrf2 pathways but not the ERK or JNK pathways [70]. HNF4α, constitutive androstane receptor (CAR), and pregnane X receptor (PXR) are the main transcription factors associated with UGT1A6 expression and activity in the liver [27,71]. However, in U251 cells, ammonia had no significant effect on *AHR*, *PXR*, *CAR*, and *Nrf2* mRNA expression (Fig. S3A) and Nrf2 protein expression (Fig. S3B). Meanwhile, neither omeprazole (AHR agonist), rifampicin (PXR agonist), nor TCPOBOP (CAR agonist) could reverse the ammonia-mediated UGT1A6 activity decline (Figs. S3C and D), and rifampicin even tended to aggravate ammonia damage to UGT1A6 activity (Fig. S3C), excluding the roles of the above receptors in brain UGT1A6 regulation in astrocytes. The tissue specificity of the regulation of UGT1A6 expression may be affected by various factors, such as receptor expression abundance and promoter distribution. The promoter of UGT1A6 contains three TATA boxes that function in a cell type-specific manner. All three TATA boxes are active in the human liver, whilst differential use of these TATA boxes has been reported in Caco-2 and lung carcinoma A549 cells [72].

Notably, we found that silencing HNF4α significantly reduced UGT1A6 protein levels and promoter activity in U251 cells, while overexpressing HNF4α increased *Ugt1a6* promoter activity. These results explain the positive correlation between HNF4α and UGT1A6 expression levels [27]. We also observed that treatment with the ERK activator TBHQ significantly decreased HNF4α protein levels in U251 cells. Other researchers also found similar results: the ERK inhibitor PD98059 increases HNF4α mRNA and protein levels in HepG2 cells [43]. In U251 cells, we further found that NH_4Cl treatment downregulated HNF4α and UGT1A6 expression levels, which could be reversed by ERK pathway inhibitor U0126, suggesting the essential role of HNF4α in the ammonia-ROS-ERK-pathway-activation-mediated decreases in UGT1A6 expression and activity. Our previous studies have found that PXR activation downregulates HNF4α in hepatocytes [39], which explains why rifampicin failed to reverse the ammonia-mediated decrease in

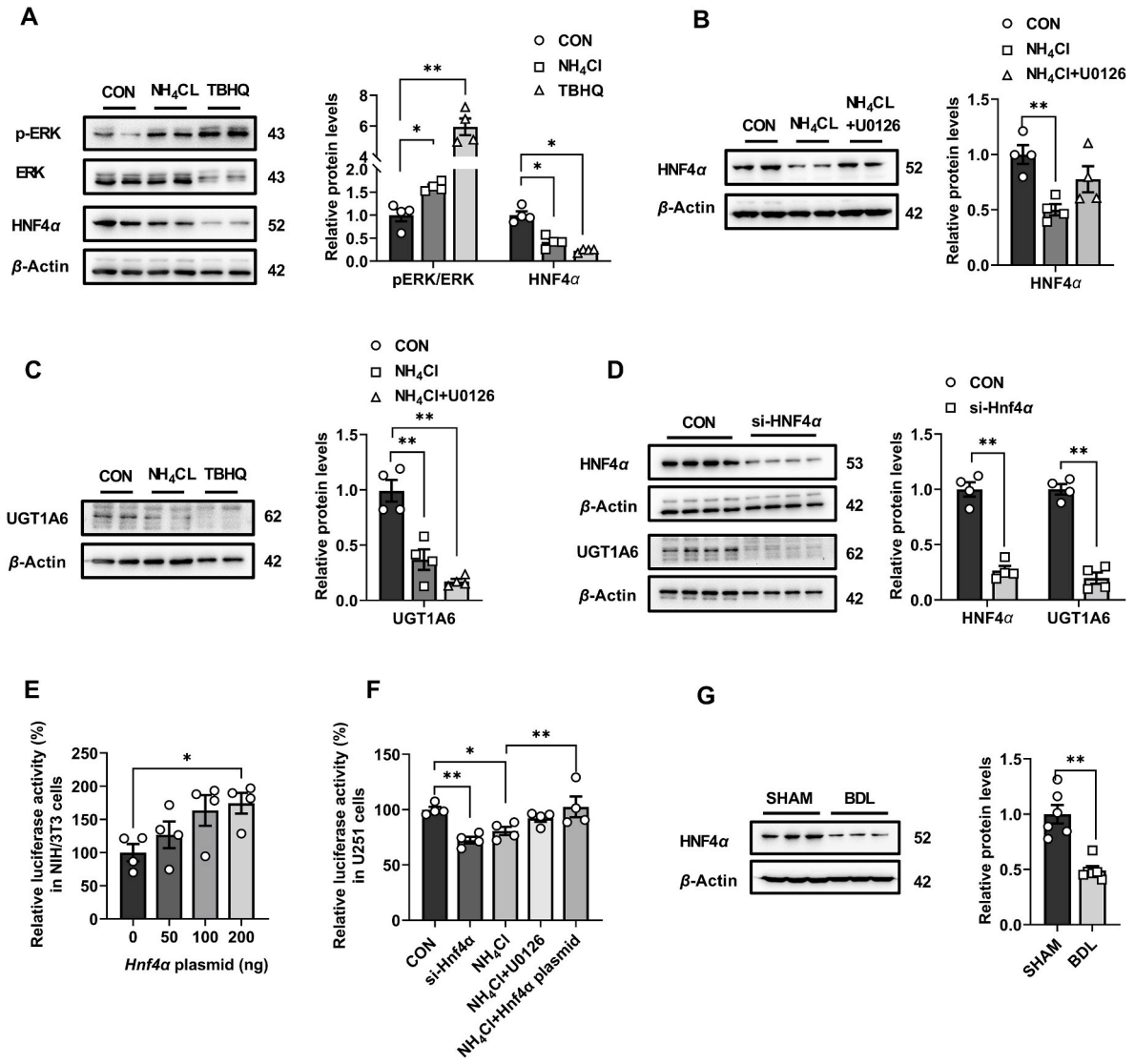

Fig. 7. Association of HNF4α with reduction in UGT1A6 expression by ROS-ERK pathway activation. Protein levels of p-ERK, HNF4α (A), and UGT1A6 (C) in U251 cells under the treatment of NH_4Cl and TBHQ. Effects of U0126 (B) on NH_4Cl-mediated decrease in HNF4α protein levels in U251 cells. Effects of silencing HNF4α on UGT1A6 protein expression in U251 cells (D). Hnf4α plasmid dose-dependently activated *Ugt1a6* promoter in NIH/3T3 cells (E). Relative *Ugt1a6* promoter luciferase reporter activity in U251 cells treated with NH_4Cl, U0126, 200 ng Hnf4α plasmid, or silenced HNF4α for 72 h (F). HNF4α protein levels in cortex of BDL and SHAM rats (G). Data are expressed as mean ± SEM (n = 4 for A-F; n = 6 for G). $^{*}P < 0.05$, $^{**}P < 0.01$.

UGT1A6 activity, further enhancing it.

To systematically prove the above findings, we generated HA rats and found they showed manic-like symptoms similar to those observed in BDL rats. Meanwhile, induced oxidative stress, the activated ROS-ERK pathway, and decreased HNF4α and UGT1A6 expression levels were also found in the cortex of HA rats, corresponding to decreased UGT1A6 activity and increased 5-HT levels. To date, all the evidence has been linked. BDL-induced HE rats showed typical manic-like behaviors accompanied by increased cortical 5-HT levels. Intraperitoneal injection of 5-HTP or i.c.v. injection of UGT1A6 inhibitor significantly increased 5-HT levels in the rat cortex and induced HE-like symptoms. Mechanistic studies confirmed that ammonia reduced UGT1A6 expression and function due to the ROS-ERK-pathway-activation-mediated reduction in HNF4α expression. These results revealed the mechanism of elevated cerebral 5-HT concentration in BDL rats and elucidated its association with manic-like behaviors in HE.

CRediT authorship contribution statement

Hanyu Yang: Conceptualization, Data curation, Investigation, Methodology, Validation, Writing – original draft. **Linjun You:** Data curation, Investigation, Methodology. **Zhongyan Wang:** Data curation, Investigation, Methodology. **Lu Yang:** Data curation, Investigation, Methodology. **Xun Wang:** Data curation, Investigation, Methodology. **Wenhan Wu:** Data curation, Investigation, Methodology. **Hao Zhi:** Data curation, Investigation, Methodology. **Guangmei Rong:** Data curation, Investigation, Methodology. **Yun Sheng:** Data curation, Investigation, Methodology. **Xiaodong Liu:** Conceptualization, Supervision, Writing – review & editing. **Li Liu:** Conceptualization, Supervision, Writing – review & editing.

Declaration of competing interest

There are no conflicts of interest to declare.

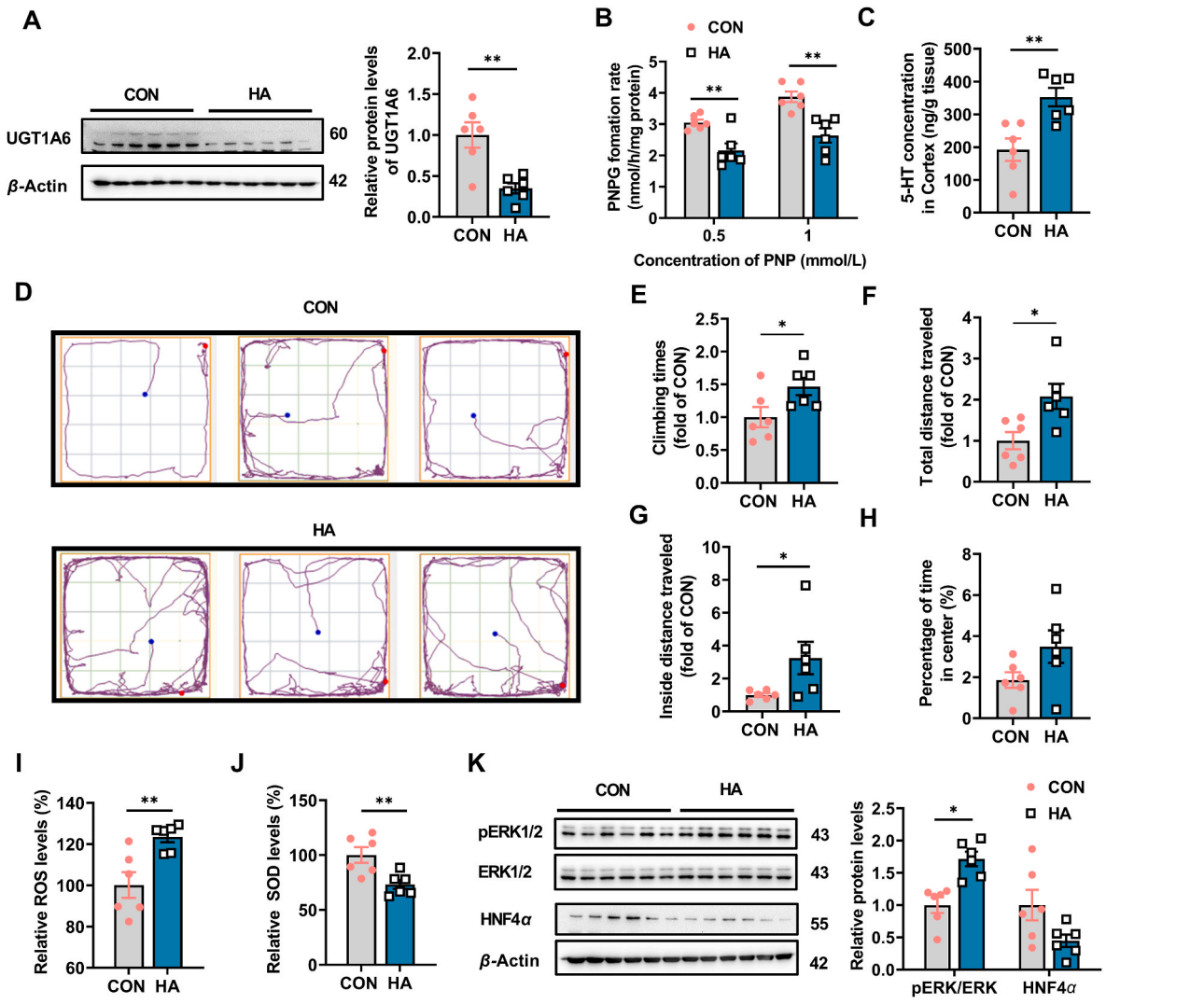

Fig. 8. Ammonia-induced oxidative stress decreased UGT1A6 activity and expression to elevate 5-HT content by activating ROS-ERK pathway in the cortex of rats. Protein levels of UGT1A6 (A) in the cortex of hyperammonemia (HA) and CON rats. Formation rate of PNPG (B) for microsomes of the cortex of HA and CON rats. Concentrations of 5-HT in the cortex of HA and CON rats (C). Track diagram (D), climbing times (E), total distance traveled (F), inside distance traveled (G), and percentage of time in center (H) of CON and HA rats in open-field test. Relative ROS (I) and SOD (J) levels, and protein levels of p-ERK and HNF4α (K) in cortices of HA and CON rats. Data are expressed as mean ± SEM (n = 6) $^{*}P < 0.05$, $^{**}P < 0.01$.

Data availability

Data will be made available on request.

Acknowledgments

This work was supported by the National Natural Science Foundation of China (Nos. 82204511, 82173884, and 82073922), the "Double First-Class" university project (No. CPU2022QZ21), the Jiangsu Funding Program for Excellent Postdoctoral Talent (No. 2022ZB305), and China Postdoctoral Science Foundation (No. 2023M733897).

Appendix A. Supplementary data

Supplementary data to this article can be found online at https://doi.org/10.1016/j.redox.2023.103019.

References

[1] D. Suraweera, V. Sundaram, S. Saab, Evaluation and management of hepatic encephalopathy: current status and future directions, Gut Liver 10 (2016) 509–519, https://doi.org/10.5009/gnl15419.
[2] K.R. Patidar, J.S. Bajaj, Covert and overt hepatic encephalopathy: diagnosis and management, Clin. Gastroenterol. Hepatol. Off. Clin. Pract. J. Am. Gastroenterol. Assoc. 13 (2015) 2048–2061, https://doi.org/10.1016/j.cgh.2015.06.039.
[3] A.R. Jayakumar, M.D. Norenberg, Endothelial-astrocytic interactions in acute liver failure, Metab. Brain Dis. 28 (2013) 183–186, https://doi.org/10.1007/s11011-012-9344-4.
[4] K. Lu, Cellular pathogenesis of hepatic encephalopathy: an update, Biomolecules 13 (2023) 396, https://doi.org/10.3390/biom13020396.
[5] E.F.M. Wijdicks, Hepatic encephalopathy, N. Engl. J. Med. 375 (2016) 1660–1670, https://doi.org/10.1056/NEJMra1600561.
[6] M.A. Bunin, R.M. Wightman, Paracrine neurotransmission in the CNS: involvement of 5-HT, Trends Neurosci. 22 (1999) 377–382, https://doi.org/10.1016/s0166-2236(99)01410-1.
[7] S. Butini, K. Nikolic, S. Kassel, H. Brückmann, S. Filipic, D. Agbaba, S. Gemma, S. Brogi, M. Brindisi, G. Campiani, H. Stark, Polypharmacology of dopamine receptor ligands, Prog. Neurobiol. 142 (2016) 68–103, https://doi.org/10.1016/j.pneurobio.2016.03.011.
[8] J. Borg, J.M. Warter, J.L. Schlienger, M. Imler, C. Marescaux, G. Mack, Neurotransmitter modifications in human cerebrospinal fluid and serum during hepatic encephalopathy, J. Neurol. Sci. 57 (1982) 343–356, https://doi.org/10.1016/0022-510x(82)90040-5.

[9] W. Kong, X. Sun, S. Yu, P. Liu, X. Zheng, J. Zhang, L. Zhu, T. Jiang, M. Jin, J. Gao, X. Fan, X. Liu, L. Liu, Bile duct ligation increased dopamine levels in the cerebral cortex of rats partly due to induction of tyrosine hydroxylase, Br. J. Pharmacol. (2023), https://doi.org/10.1111/bph.16041.
[10] N. Mikkelsen, P. Damkier, S.A. Pedersen, Serotonin syndrome—a focused review, Basic Clin. Pharmacol. Toxicol. 133 (2023) 124–129, https://doi.org/10.1111/bcpt.13912.
[11] M. Pourhamzeh, F.G. Moravej, M. Arabi, E. Shahriari, S. Mehrabi, R. Ward, R. Ahadi, M.T. Joghataei, The roles of serotonin in neuropsychiatric disorders, Cell. Mol. Neurobiol. 42 (2022) 1671–1692, https://doi.org/10.1007/s10571-021-01064-9.
[12] D.J. Walther, J.-U. Peter, S. Bashammakh, H. Hörtnagl, M. Voits, H. Fink, M. Bader, Synthesis of serotonin by a second tryptophan hydroxylase isoform, Science 299 (2003), https://doi.org/10.1126/science.1078197, 76–76.
[13] S.M. Berger, T. Weber, S. Perreau-Lenz, M.A. Vogt, S.E. Gartside, C. Maser-Gluth, L. Lanfumey, P. Gass, R. Spanagel, D. Bartsch, A functional Tph2 C1473G polymorphism causes an anxiety phenotype via compensatory changes in the serotonergic system, Neuropsychopharmacol. Off. Publ. Am. Coll. Neuropsychopharmacol. 37 (2012) 1986–1998, https://doi.org/10.1038/npp.2012.46.
[14] V.L. Rao, J.F. Giguère, G.P. Layrargues, R.F. Butterworth, Increased activities of MAOA and MAOB in autopsied brain tissue from cirrhotic patients with hepatic encephalopathy, Brain Res. 621 (1993) 349–352, https://doi.org/10.1016/0006-8993(93)90126-8.
[15] D.D. Mousseau, G.B. Baker, R.F. Butterworth, Increased density of catalytic sites and expression of brain monoamine oxidase A in humans with hepatic encephalopathy, J. Neurochem. 68 (1997) 1200–1208, https://doi.org/10.1046/j.1471-4159.1997.68031200.x.
[16] H. Weissbach, W. Lovenberg, B.G. Redfield, S. Udenfriend, In vivo metabolism of serotonin and tryptamine: effect of monoamine oxidase inhibition, J. Pharmacol. Exp. Therapeut. 131 (1961) 26–30.
[17] M. Ouzzine, S. Gulberti, N. Ramalanjaona, J. Magdalou, S. Fournel-Gigleux, The UDP-glucuronosyltransferases of the blood-brain barrier: their role in drug metabolism and detoxication, Front. Cell. Neurosci. 8 (2014) 349, https://doi.org/10.3389/fncel.2014.00349.
[18] C.D. King, G.R. Rios, J.A. Assouline, T.R. Tephly, Expression of UDP-glucuronosyltransferases (UGTs) 2B7 and 1A6 in the human brain and identification of 5-hydroxytryptamine as a substrate, Arch. Biochem. Biophys. 365 (1999) 156–162, https://doi.org/10.1006/abbi.1999.1155.
[19] S. Krishnaswamy, S.X. Duan, L.L. Von Moltke, D.J. Greenblatt, M.H. Court, Validation of serotonin (5-hydroxtryptamine) as an in vitro substrate probe for human UDP-glucuronosyltransferase (UGT) 1A6, Drug Metab. Dispos. Biol. Fate Chem. 31 (2003) 133–139, https://doi.org/10.1124/dmd.31.1.133.
[20] S. Ohno, S. Nakajin, Determination of mRNA expression of human UDP-glucuronosyltransferases and application for localization in various human tissues by real-time reverse transcriptase-polymerase chain reaction, Drug Metab. Dispos. 37 (2009) 32–40, https://doi.org/10.1124/dmd.108.023598.
[21] M.H. Court, X. Zhang, X. Ding, K.K. Yee, L.M. Hesse, M. Finel, Quantitative distribution of mRNAs encoding the 19 human UDP-glucuronosyltransferase enzymes in 26 adult and 3 fetal tissues, Xenobiotica Fate Foreign Compd. Biol. Syst. 42 (2012) 266–277, https://doi.org/10.3109/00498254.2011.618954.
[22] T. Suominen, P. Uutela, R.A. Ketola, J. Bergquist, L. Hillered, M. Finel, H. Zhang, A. Laakso, R. Kostiainen, Determination of serotonin and dopamine metabolites in human brain Microdialysis and cerebrospinal fluid samples by UPLC-MS/MS: discovery of intact glucuronide and sulfate conjugates, PLoS One 8 (2013), e68007, https://doi.org/10.1371/journal.pone.0068007.
[23] P. Uutela, R. Reinilä, K. Harju, P. Piepponen, R.A. Ketola, R. Kostiainen, Analysis of intact glucuronides and sulfates of serotonin, dopamine, and their phase I metabolites in rat brain microdialysates by liquid chromatography-tandem mass spectrometry, Anal. Chem. 81 (2009) 8417–8425, https://doi.org/10.1021/ac901320z.
[24] A. Wajda, J. Łapczuk, M. Grabowska, M. Słojewski, M. Laszczyńska, E. Urasińska, M. Droździk, Nuclear factor E2-related factor-2 (Nrf2) expression and regulation in male reproductive tract, Pharmacol. Rep. 68 (2016) 101–108, https://doi.org/10.1016/j.pharep.2015.07.005.
[25] R. Meech, D.G. Hu, R.A. McKinnon, S.N. Mubarokah, A.Z. Haines, P.C. Nair, A. Rowland, P.I. Mackenzie, The UDP-glycosyltransferase (UGT) superfamily: new members, new functions, and novel paradigms, Physiol. Rev. 99 (2019) 1153–1222, https://doi.org/10.1152/physrev.00058.2017.
[26] Y. Emi, S. Ikushiro, T. Iyanagi, Xenobiotic responsive element-mediated transcriptional activation in the UDP-glucuronosyltransferase family 1 gene complex, J. Biol. Chem. 271 (1996) 3952–3958, https://doi.org/10.1074/jbc.271.7.3952.
[27] S. Aueviriyavit, T. Furihata, K. Morimoto, K. Kobayashi, K. Chiba, Hepatocyte nuclear factor 1 alpha and 4 alpha are factors involved in interindividual variability in the expression of UGT1A6 and UGT1A9 but not UGT1A1, UGT1A3 and UGT1A4 mRNA in human livers, Drug Metabol. Pharmacokinet. 22 (2007) 391–398, https://doi.org/10.2133/dmpk.22.391.
[28] C. Köhle, O.A. Badary, K. Nill, B.S. Bock-Hennig, K.W. Bock, Serotonin glucuronidation by Ah receptor- and oxidative stress-inducible human UDP-glucuronosyltransferase (UGT) 1A6 in Caco-2 cells, Biochem. Pharmacol. 69 (2005) 1397–1402, https://doi.org/10.1016/j.bcp.2005.02.010.
[29] T. Weiss-Sadan, M. Ge, M. Hayashi, M. Gohar, C.-H. Yao, A. de Groot, S. Harry, A. Carlin, H. Fischer, L. Shi, T.-Y. Wei, C.H. Adelmann, K. Wolf, T. Vornbäumen, B. R. Dürr, M. Takahashi, M. Richter, J. Zhang, T.-Y. Yang, V. Vijay, D.E. Fisher, A. N. Hata, M.C. Haigis, R. Mostoslavsky, N. Bardeesy, T. Papagiannakopoulos, L. Bar-Peled, NRF2 activation induces NADH-reductive stress, providing a metabolic vulnerability in lung cancer, Cell Metabol. 35 (2023) 487–503.e7, https://doi.org/10.1016/j.cmet.2023.01.012.
[30] R.L. Yeager, S.A. Reisman, L.M. Aleksunes, C.D. Klaassen, Introducing the "TCDD-inducible AhR-Nrf2 gene battery,", Toxicol. Sci. Off. J. Soc. Toxicol. 111 (2009) 238–246, https://doi.org/10.1093/toxsci/kfp115.
[31] T. Heurtaux, A. Benani, A. Bianchi, A. Moindrot, D. Gradinaru, J. Magdalou, P. Netter, A. Minn, Redox state alteration modulates astrocyte glucuronidation, Free Radic. Biol. Med. 37 (2004) 1051–1063, https://doi.org/10.1016/j.freeradbiomed.2004.06.020.
[32] D. Gradinaru, A.-L. Minn, Y. Artur, A. Minn, J.-M. Heydel, Effect of oxidative stress on UDP-glucuronosyltransferases in rat astrocytes, Toxicol. Lett. 213 (2012) 316–324, https://doi.org/10.1016/j.toxlet.2012.07.014.
[33] Y. Li, J. Zhang, P. Xu, B. Sun, Z. Zhong, C. Liu, Z. Ling, Y. Chen, N. Shu, K. Zhao, L. Liu, X. Liu, Acute liver failure impairs function and expression of breast cancer-resistant protein (BCRP) at rat blood-brain barrier partly via ammonia-ROS-ERK1/2 activation, J. Neurochem. 138 (2016) 282–294, https://doi.org/10.1111/jnc.13666.
[34] E. Kosenko, N. Venediktova, Y. Kaminsky, C. Montoliu, V. Felipo, Sources of oxygen radicals in brain in acute ammonia intoxication in vivo, Brain Res. 981 (2003) 193–200, https://doi.org/10.1016/s0006-8993(03)03035-x.
[35] E. Kosenko, Y. Kaminsky, A. Kaminsky, M. Valencia, L. Lee, C. Hermenegildo, V. Felipo, Superoxide production and antioxidant enzymes in ammonia intoxication in rats, Free Radic. Res. 27 (1997) 637–644, https://doi.org/10.3109/10715769709097867.
[36] J. Kountouras, B.H. Billing, P.J. Scheuer, Prolonged bile duct obstruction: a new experimental model for cirrhosis in the rat, Br. J. Exp. Pathol. 65 (1984) 305–311.
[37] M. Rysz, E. Bromek, W.A. Daniel, Activation of brain serotonergic system by repeated intracerebral administration of 5-hydroxytryptophan (5-HTP) decreases the expression and activity of liver cytochrome P450, Biochem. Pharmacol. 99 (2016) 113–122, https://doi.org/10.1016/j.bcp.2015.11.014.
[38] L. Zhu, H. Zhou, F. Xu, H. Yang, P. Li, Y. Sheng, P. Liu, W. Kong, X. Liu, L. Yang, L. Liu, X. Liu, Hepatic ischemia-reperfusion impairs blood-brain barrier partly due to release of arginase from injured liver, Front. Pharmacol. 12 (2021), https://doi.org/10.3389/fphar.2021.724471.
[39] P. Liu, L. Jiang, W. Kong, Q. Xie, P. Li, X. Liu, J. Zhang, M. Liu, Z. Wang, L. Zhu, H. Yang, Y. Zhou, J. Zou, X. Liu, L. Liu, PXR activation impairs hepatic glucose metabolism partly via inhibiting the HNF4α–GLUT2 pathway, Acta Pharm. Sin. B 12 (2022) 2391–2405, https://doi.org/10.1016/j.apsb.2021.09.031.
[40] H. Yang, M. Su, M. Liu, Y. Sheng, L. Zhu, L. Yang, R. Mu, J. Zou, X. Liu, L. Liu, Hepatic retinaldehyde deficiency is involved in diabetes deterioration by enhancing PCK1- and G6PC-mediated gluconeogenesis, Acta Pharm. Sin. B 13 (2023) 3728–3743, https://doi.org/10.1016/j.apsb.2023.06.014.
[41] Q. Han, A. Wang, Q. Fu, S. Zhou, J. Bao, H. Xing, Protective role of selenium on ammonia-mediated nephrotoxicity via PI3K/AKT/mTOR pathway: crosstalk between autophagy and cytokine release, Ecotoxicol. Environ. Saf. 242 (2022), 113918, https://doi.org/10.1016/j.ecoenv.2022.113918.
[42] P. Zheng, X. Qin, R. Feng, Q. Li, F. Huang, Y. Li, Q. Zhao, H. Huang, Alleviative effect of melatonin on the decrease of uterine receptivity caused by blood ammonia through ROS/NF-κB pathway in dairy cow, Ecotoxicol. Environ. Saf. 231 (2022), 113166, https://doi.org/10.1016/j.ecoenv.2022.113166.
[43] S. Reddy, W. Yang, D.G. Taylor, X. q Shen, D. Oxender, G. Kust, T. Leff, Mitogen-activated protein kinase regulates transcription of the ApoCIII gene. Involvement of the orphan nuclear receptor HNF4, J. Biol. Chem. 274 (1999) 33050–33056, https://doi.org/10.1074/jbc.274.46.33050.
[44] C. Yurdaydin, H. Hörtnagl, P. Steindl, C. Zimmermann, C. Pifl, E.A. Singer, E. Roth, P. Ferenci, Increased serotoninergic and noradrenergic activity in hepatic encephalopathy in rats with thioacetamide-induced acute liver failure, Hepatol. Baltim. Md 12 (1990) 695–700, https://doi.org/10.1002/hep.1840120413.
[45] M. Eftekar, The association between hepatic encephalopathy/minimal hepatic encephalopathy and depressive and anxiety disorders: a systematic review, Australas. Psychiatr. 28 (2020) 61–65, https://doi.org/10.1177/1039856219875054.
[46] Y. Bai, K. Li, X. Li, X. Chen, J. Zheng, F. Wu, J. Chen, Z. Li, S. Zhang, K. Wu, Y. Chen, Y. Wang, Y. Yang, Effects of oxidative stress on hepatic encephalopathy pathogenesis in mice, Nat. Commun. 14 (2023) 4456, https://doi.org/10.1038/s41467-023-40081-8.
[47] W.F. Byerley, L.L. Judd, F.W. Reimherr, B.I. Grosser, 5-Hydroxytryptophan: a review of its antidepressant efficacy and adverse effects, J. Clin. Psychopharmacol. 7 (1987) 127–137.
[48] K. Nisijima, T. Yoshino, K. Yui, S. Katoh, Potent serotonin (5-HT)2A receptor antagonists completely prevent the development of hyperthermia in an animal model of the 5-HT syndrome, Brain Res. 890 (2001) 23–31, https://doi.org/10.1016/S0006-8993(00)03020-1.
[49] J. Ren, D. Friedmann, J. Xiong, C.D. Liu, B.R. Ferguson, T. Weerakkody, K. E. DeLoach, C. Ran, A. Pun, Y. Sun, B. Weissbourd, R.L. Neve, J. Huguenard, M. A. Horowitz, L. Luo, Anatomically defined and functionally distinct dorsal raphe serotonin sub-systems, Cell 175 (2018) 472–487.e20, https://doi.org/10.1016/j.cell.2018.07.043.
[50] L.G. Chia, D.R. Ni, F.C. Cheng, Y.P. Ho, J.S. Kuo, Intrastriatal injection of 5,7-dihydroxytryptamine decreased 5-HT levels in the striatum and suppressed locomotor activity in C57BL/6 mice, Neurochem. Res. 24 (1999) 719–722, https://doi.org/10.1023/a:1020771211305.
[51] F. Moroni, G. Lombardi, V. Carlà, S. Lal, P. Etienne, N.P. Nair, Increase in the content of quinolinic acid in cerebrospinal fluid and frontal cortex of patients with

hepatic failure, J. Neurochem. 47 (1986) 1667–1671, https://doi.org/10.1111/j.1471-4159.1986.tb13071.x.
[52] S.J. Kish, Y. Furukawa, L.-J. Chang, J. Tong, N. Ginovart, A. Wilson, S. Houle, J. H. Meyer, Regional distribution of serotonin transporter protein in postmortem human brain: is the cerebellum a SERT-free brain region? Nucl. Med. Biol. 32 (2005) 123–128, https://doi.org/10.1016/j.nucmedbio.2004.10.001.
[53] W.-S. Huang, S.-Y. Huang, P.-S. Ho, K.-H. Ma, Y.-Y. Huang, C.-B. Yeh, R.-S. Liu, C.-Y. Cheng, C.-Y. Shiue, PET imaging of the brain serotonin transporters (SERT) with N,N-dimethyl-2-(2-amino-4-[18F]fluorophenylthio)benzylamine (4-[18F]-ADAM) in humans: a preliminary study, Eur. J. Nucl. Med. Mol. Imag. 40 (2013) 115–124, https://doi.org/10.1007/s00259-012-2250-5.
[54] A. Michalak, N. Chatauret, R.F. Butterworth, Evidence for a serotonin transporter deficit in experimental acute liver failure, Neurochem. Int. 38 (2001) 163–168, https://doi.org/10.1016/s0197-0186(00)00062-0.
[55] K.G. Baker, G.M. Halliday, P. Halasz, J.P. Hornung, L.B. Geffen, R.G. Cotton, I. Törk, Cytoarchitecture of serotonin-synthesizing neurons in the pontine tegmentum of the human brain, Synap. N. Y. N. 7 (1991) 301–320, https://doi.org/10.1002/syn.890070407.
[56] G.M. Halliday, Y.W. Li, T.H. Joh, R.G. Cotton, P.R. Howe, L.B. Geffen, W. W. Blessing, Distribution of monoamine-synthesizing neurons in the human medulla oblongata, J. Comp. Neurol. 273 (1988) 301–317, https://doi.org/10.1002/cne.902730303.
[57] F.G. Suleman, A. Abid, D. Gradinaru, J.L. Daval, J. Magdalou, A. Minn, Identification of the uridine diphosphate glucuronosyltransferase isoform UGT1A6 in rat brain and in primary cultures of neurons and astrocytes, Arch. Biochem. Biophys. 358 (1998) 63–67, https://doi.org/10.1006/abbi.1998.0842.
[58] R.F. Butterworth, Pathophysiology of hepatic encephalopathy: a new look at ammonia, Metab. Brain Dis. 17 (2002) 221–227, https://doi.org/10.1023/a:1021989230535.
[59] I. Zemtsova, B. Görg, V. Keitel, H.-J. Bidmon, K. Schrör, D. Häussinger, Microglia activation in hepatic encephalopathy in rats and humans, Hepatol. Baltim. Md 54 (2011) 204–215, https://doi.org/10.1002/hep.24326.
[60] X.-M. Liu, K.J. Peyton, W. Durante, Ammonia promotes endothelial cell survival via the heme oxygenase-1-mediated release of carbon monoxide, Free Radic. Biol. Med. 102 (2017) 37–46, https://doi.org/10.1016/j.freeradbiomed.2016.11.029.
[61] S.L. Forrest, J.H. Kim, D.R. Crockford, K. Huynh, R. Cheong, S. Knott, M.A. Kane, L. M. Ittner, G.M. Halliday, J.J. Kril, Distribution patterns of astrocyte populations in the human cortex, Neurochem. Res. 48 (2023) 1222–1232, https://doi.org/10.1007/s11064-022-03700-2.
[62] N.E. Piloni, V. Fermandez, L.A. Videla, S. Puntarulo, Acute iron overload and oxidative stress in brain, Toxicology 314 (2013) 174–182, https://doi.org/10.1016/j.tox.2013.09.015.
[63] L. Radenovic, M. Nenadic, M. Ułamek-Kozioł, S. Januszewski, S.J. Czuczwar, P. R. Andjus, R. Pluta, Heterogeneity in brain distribution of activated microglia and astrocytes in a rat ischemic model of Alzheimer's disease after 2 years of survival, Aging 12 (2020) 12251–12267, https://doi.org/10.18632/aging.103411.
[64] M. Węgrzynowicz, W. Hilgier, A. Dybel, S.S. Oja, P. Saransaari, J. Albrecht, Upregulation of cerebral cortical glutathione synthesis by ammonia in vivo and in cultured glial cells: the role of cystine uptake, Neurochem. Int. 50 (2007) 883–889, https://doi.org/10.1016/j.neuint.2006.12.003.
[65] V. Beray-Berthat, N. Croci, M. Plotkine, I. Margaill, Polymorphonuclear neutrophils contribute to infarction and oxidative stress in the cortex but not in the striatum after ischemia–reperfusion in rats, Brain Res. 987 (2003) 32–38, https://doi.org/10.1016/S0006-8993(03)03224-4.
[66] O. Rodriguez-Mora, M.M. LaHair, C.J. Howe, J.A. McCubrey, R.A. Franklin, Calcium/calmodulin-dependent protein kinases as potential targets in cancer therapy, Expert Opin. Ther. Targets 9 (2005) 791–808, https://doi.org/10.1517/14728222.9.4.791.
[67] J.A. McCubrey, M.M. Lahair, R.A. Franklin, Reactive oxygen species-induced activation of the MAP kinase signaling pathways, Antioxidants Redox Signal. 8 (2006) 1775–1789, https://doi.org/10.1089/ars.2006.8.1775.
[68] J.A. McCubrey, S.L. Abrams, G. Ligresti, N. Misaghian, E.W.T. Wong, L. S. Steelman, J. Bäsecke, J. Troppmair, M. Libra, F. Nicoletti, S. Molton, M. McMahon, C. Evangelisti, A.M. Martelli, Involvement of p53 and Raf/MEK/ERK pathways in hematopoietic drug resistance, Leukemia 22 (2008) 2080–2090, https://doi.org/10.1038/leu.2008.207.
[69] A.R. Jayakumar, X.Y. Tong, K.M. Curtis, R. Ruiz-Cordero, M.T. Abreu, M. D. Norenberg, Increased toll-like receptor 4 in cerebral endothelial cells contributes to the astrocyte swelling and brain edema in acute hepatic encephalopathy, J. Neurochem. 128 (2014) 890–903, https://doi.org/10.1111/jnc.12516.
[70] Y. Sakakibara, A. Kojima, Y. Asai, M. Nadai, M. Katoh, Changes in uridine 5′-diphospho-glucuronosyltransferase 1A6 expression by histone deacetylase inhibitor valproic acid, Biopharm. Drug Dispos. 43 (2022) 175–182, https://doi.org/10.1002/bdd.2328.
[71] E. Neumann, H. Mehboob, J. Ramírez, S. Mirkov, M. Zhang, W. Liu, Age-dependent hepatic UDP-glucuronosyltransferase gene expression and activity in children, Front. Pharmacol. 7 (2016), https://doi.org/10.3389/fphar.2016.00437.
[72] P.A. Münzel, T. Lehmköster, M. Brück, J.K. Ritter, K.W. Bock, Aryl hydrocarbon receptor-inducible or constitutive expression of human UDP glucuronosyltransferase UGT1A6, Arch. Biochem. Biophys. 350 (1998) 72–78, https://doi.org/10.1006/abbi.1997.0485.